Research Paper
J. Astron. Space Sci. 27(2), 81-88 (2010)
DOI: 10.5140/JASS.2010.27.2.081

JASS Journal of Astronomy and Space Sciences

Photometric Observations of the Contact Binary System V523 Cassiopeiae

Jang Hae Jeong[1,2†], Chun-Hwey Kim[1,2], and Yong-Sam Lee[1,2]

[1]Department of Astronomy and Space Science, Chungbuk National University, Cheongju 361-763, Korea
[2]Chungbuk National University Observatory, Cheongju 361-763, Korea

A total of 583 observations (193 in Δb, 190 in Δv, 200 in Δr) for V523 Cas was made on 9 nights from September to December in 2008 using the 100 cm telescope with 2K CCD camera of the Chungbuk National University Observatory. With our data *BVR* light curves were constructed and 9 times of minimum light were determined. We also obtained physical parameters of the V523 Cas system by analysis of the *BVR* light curves using the Wilson-Devinney code.

Keywords: *BVR* observations, times of minimum light, V523 Cas, Wilson-Devinney solution

1. INTRODUCTION

V523 Cassiopeiae (Wr16, CSV5867, GSC 3257-167) is a W-type W UMa eclipsing binary system (the smaller is hotter; see Hendry & Mochnacki 2000). Since Weber (1958) discovered the light variability of V523 Cas, many investigations in photometry and spectroscopy have been carried out (Zhukov 1972, Haussler 1974, Lavrov & Zhukov 1975, Bradstreet 1981, Hoffmann 1981, Samec & Bookmyer 1987, Zhai et al. 1988, Samec et al. 1989, Kim & Jeong 2002, Samec et al. 2004, Genet et al. 2005, Jeong et al. 2006). In results, some facts about V523 Cas are known: 1) its orbital period of about 336 minutes is one of the shortest among late type contact binaries. 2) Its light curves show a relatively deep eclipse (~$0.^{m}8$) and probably total at primary eclipse. 3) V523 Cas is noted for variations in its light curve, for rapid changes in photometric light-curve asymmetries, and also for large orbital period changes.

Each component of the V523 Cas system is rapidly rotating compared to most late single stars. It may cause magnetically active phenomena. Genet et al. (2005) tried to determine small changes in rotational periods from one season to the next, with considerable precision. They explained that such small changes in rotational periods can be caused by mass loss, the transfer of mass from one star to the other, or the Applegate (1992) effect. Also they suggested third bodies can induce changes in eclipse epoch due to the light-travel-time effect resulting from the system shifting barycenter.

Samec & Bookmyer (1987) and Samec et al. (1989) reviewed the early history of this system. Mass ratios produced by photometric solutions of V523 Cas are q_{ph} = 0.59 by Bradstreet (1981), 0.571 by Samec et al. (1989), 0.53 by Lister et al. (2000), 0.56 by Kim & Jeong (2002), and 0.52 by Samec et al. (2004). Those values disagreed with the spectroscopic mass ratio, q_{sp} = 0.42, derived directly from radial velocity curves by Milone et al. (1985). Niarchos & Duerbeck (1991) had proposed that a circulation effect of sideward convection may affect the radial velocity curves in a systematic way, causing the discrepancy in q_{ph} and q_{sp}. However, an analysis of new, high-precision radial velocity curves by Rucinski et al. (2003) has shown that q_{sp} = 0.512. Samec et al. (2004) found that, even with using simultaneous solution method, it is impossible to get a good fit to the light curve and the radial velocity curves.

Received April 20, 2010 **Accepted** May 25, 2010

†**Corresponding Author**
E-mail: jeongjh@chungbuk.ac.kr
Tel: +82-43-261-2313 Fax: +82-43-274-2312

Jeong et al. (2006) obtained q = 0.54 from the combined analysis of their *BVRI* light curves with the double-lined radial velocity curves of Rucinski et al. (2003) by the Wilson-Devinney (WD) binary model.

Even the problem of the difference between two kinds of q values vanished somewhat, but for the problems of the light variability and the period changes we need obtain high-precision light curves for the analysis of light-curve periodicity of the V523 Cas system. W UMa systems are classified as A-types or W-types. In A-type systems the more massive component is covered at primary eclipse and the systems are found to be well overcontact, whereas W-type systems have the lower-mass component covered at primary eclipse and are in thin contact. The W-types are unevolved objects which cannot achieve equilibrium, while the A-types tend to be somewhat evolved, have higher total masses and thicker common envelopes (Wilson 1978). It is thought for the W-types to undergo thermal relaxation oscillations (TRO) near a state of marginal contact (Flannery 1976, Lucy 1976, Robertson & Eggleton 1977). Observation of the W-types shows that orbital period is changing and light is varying. Due to such a phenomenon, W-types are expected such objects as cannot achieve equilibrium. V523 Cas is a member of the W-type W UMa class. To explain the observational behaviors for W UMa binaries, often adopted

Table 1. B observations of V523 Cas in 2008.

$JD_\odot$ 2450300+	ΔB	$JD_\odot$ 2450300+	ΔB	$JD_\odot$ 2450300+	ΔB	$JD_\odot$ 2450300+	ΔB	$JD_\odot$ 2450300+	ΔB
739.0915	-1.837	743.0931	-1.713	767.1417	-1.808	774.1619	-1.811	802.1477	-1.372
739.1023	-1.820	743.1256	-0.860	767.1445	-1.832	774.1685	-1.772	802.1507	-1.423
739.1086	-1.800	743.1378	-0.977	767.1529	-1.785	774.1769	-1.697	802.1536	-1.550
739.1118	-1.794	758.0486	-1.709	767.1642	-1.697	774.2075	-0.883	802.1576	-1.582
739.1149	-1.753	758.0518	-1.654	767.1805	-1.371	774.2149	-0.879	803.0393	-1.674
739.1213	-1.711	758.0616	-1.573	767.1834	-1.300	801.9981	-1.459	803.0425	-1.662
739.1244	-1.691	758.0649	-1.480	767.1862	-1.164	802.0002	-1.404	803.0457	-1.593
739.1275	-1.635	758.0778	-0.957	767.1918	-0.947	802.0047	-1.256	803.0490	-1.548
739.1307	-1.584	758.0844	-0.865	767.1946	-0.835	802.0074	-1.150	803.0522	-1.511
739.1338	-1.534	758.0909	-0.885	767.1974	-0.805	802.0095	-1.037	803.0554	-1.431
739.1432	-1.179	758.0941	-0.936	767.2087	-1.035	802.0121	-0.930	803.0586	-1.361
739.1469	-1.073	758.0974	-1.118	767.2229	-1.481	802.0149	-0.834	803.0620	-1.246
739.1510	-0.904	758.1006	-1.244	767.2286	-1.579	802.0183	-0.820	803.0655	-1.137
739.1558	-0.861	758.1039	-1.354	770.1130	-1.210	802.0210	-0.818	803.0693	-1.095
739.2120	-1.782	758.1071	-1.401	770.1403	-1.554	802.0237	-0.839	803.0731	-1.101
741.0726	-1.728	758.1169	-1.613	770.1461	-1.608	802.0264	-0.923	803.0771	-1.193
741.0759	-1.755	758.1201	-1.656	770.1572	-1.721	802.0431	-1.503	803.0809	-1.301
741.0793	-1.768	758.1234	-1.644	770.1635	-1.819	802.0486	-1.586	803.0848	-1.399
741.0826	-1.792	758.1267	-1.751	770.2063	-1.702	802.0692	-1.767	803.0887	-1.513
741.0859	-1.744	758.1299	-1.765	770.2116	-1.592	802.0719	-1.798	803.0924	-1.570
741.0895	-1.727	758.1364	-1.783	770.2169	-1.539	802.0801	-1.806	803.0958	-1.629
741.0967	-1.746	758.1461	-1.812	770.2222	-1.293	802.0855	-1.807	803.0993	-1.696
741.1003	-1.750	758.1494	-1.817	770.2328	-0.805	802.0882	-1.800	803.1028	-1.716
741.1151	-1.635	758.1591	-1.730	770.2434	-0.900	802.0909	-1.786	803.1065	-1.744
741.1226	-1.507	758.1623	-1.724	770.2488	-1.124	802.0937	-1.758	803.1099	-1.769
741.1263	-1.411	758.1786	-1.526	774.1101	-1.469	802.0964	-1.744	803.1133	-1.808
741.1301	-1.319	758.1818	-1.505	774.1160	-1.594	802.0991	-1.733	803.1169	-1.820
741.1375	-1.081	758.1981	-1.119	774.1254	-1.717	802.1073	-1.658	803.1205	-1.839
741.1412	-1.044	758.2046	-1.098	774.1341	-1.770	802.1100	-1.623	803.1240	-1.839
741.1449	-1.065	758.2078	-1.183	774.1358	-1.794	802.1128	-1.586	803.1275	-1.861
741.1487	-1.192	758.2143	-1.319	774.1376	-1.803	802.1155	-1.546	803.1309	-1.838
741.1524	-1.259	758.2403	-1.824	774.1410	-1.811	802.1212	-1.423	803.1343	-1.823
741.1635	-1.522	767.0357	-1.745	774.1426	-1.811	802.1241	-1.352	803.1377	-1.821
742.9946	-1.472	767.0414	-1.727	774.1442	-1.828	802.1271	-1.273		
742.9989	-1.336	767.0444	-1.718	774.1457	-1.813	802.1300	-1.186		
743.0324	-1.510	767.0591	-1.574	774.1505	-1.854	802.1330	-1.124		
743.0495	-1.745	767.0822	-1.061	774.1522	-1.842	802.1359	-1.089		
743.0603	-1.788	767.0928	-1.292	774.1537	-1.850	802.1389	-1.111		
743.0650	-1.802	767.1140	-1.683	774.1553	-1.828	802.1419	-1.189		
743.0731	-1.818	767.1296	-1.797	774.1585	-1.835	802.1448	-1.261		

are a scenario as magnetic activities (as like star spots) on the late and rapidly rotating star. In the same sense we will also analyze the light curves of V523 Cas we observed.

2. OBSERVATIONS AND LIGHT CURVES

Using the 100 cm reflector equipped with 2K CCD camera system of Chungbuk National University Observatory, we observed V523 Cas on 9 nights in 2008. The stars of GSC 3257-0011 and GSC 3257-0221 are observed for comparison and check, respectively. The observations were reduced using the Image Reduction and Analysis Facility (IRAF) differential photometric method. Differential *BVR* magnitudes for all observations are standardized. All procedures for reduction and standardization we used are described in Jeong et al. (2009). A total of 583 observations in *BVR* are obtained as listed in Tables 1-3.

With our data, we determined 9 times of minimum light using the Kwee & van Woerden (1956) method, as listed in Table 4, and constructed *BVR* light curves as shown in Fig. 1. The probable errors of our data are $\pm 0.^{m}015$ in *B*, $\pm 0.^{m}019$ in *V*, and $\pm 0.^{m}019$ in *R*. Those are as shown at bottom left corner of Fig. 1. We calculated orbital phases using the light element:

Table 2. V observations of V523 Cas in 2008.

$JD_{\odot}$ 2450300+	ΔV	$JD_{\odot}$ 2450300+	ΔV	$JD_{\odot}$ 2450300+	ΔV	$JD_{\odot}$ 2450300+	ΔV	$JD_{\odot}$ 2450300+	ΔV
739.0889	-2.129	743.0986	-1.984	767.1251	-2.104	774.1605	-2.108	802.1080	-1.948
739.0926	-2.150	743.1268	-1.201	767.1305	-2.110	774.1626	-2.097	802.1107	-1.929
739.0998	-2.136	743.1391	-1.455	767.1332	-2.134	774.1657	-2.103	802.1134	-1.891
739.1094	-2.084	758.0462	-2.071	767.1361	-2.132	774.1695	-2.061	802.1161	-1.862
739.1125	-2.080	758.0494	-2.084	767.1426	-2.137	774.1737	-2.034	802.1190	-1.767
739.1220	-2.006	758.0526	-1.988	767.1454	-2.129	774.1864	-1.899	802.1219	-1.708
739.1251	-1.989	758.0657	-1.748	767.1623	-2.021	774.1911	-1.745	802.1249	-1.649
739.1282	-1.951	758.0721	-1.578	767.1651	-2.006	774.1965	-1.608	802.1279	-1.564
739.1314	-1.889	758.0787	-1.118	767.1693	-1.941	774.2027	-1.357	802.1308	-1.485
739.1345	-1.821	758.0852	-1.185	767.1722	-1.887	774.2239	-1.614	802.1338	-1.442
739.1377	-1.690	758.1112	-1.885	767.1871	-1.486	774.2312	-1.794	802.1367	-1.450
739.1439	-1.501	758.1275	-1.992	767.1899	-1.367	774.2382	-1.911	802.1397	-1.487
739.1572	-1.202	758.1307	-2.039	767.1927	-1.247	801.9987	-1.769	802.1456	-1.619
741.0768	-2.097	758.1339	-2.109	767.1955	-1.200	802.0008	-1.718	802.1485	-1.691
741.0801	-2.123	758.1372	-2.102	767.2012	-1.179	802.0030	-1.638	802.1515	-1.795
741.0834	-2.084	758.1405	-2.127	767.2068	-1.364	802.0053	-1.569	802.1544	-1.849
741.0869	-2.097	758.1437	-2.095	767.2124	-1.561	802.0128	-1.221	803.0528	-1.800
741.0904	-2.095	758.1470	-2.083	767.2153	-1.652	802.0189	-1.173	803.0664	-1.454
741.0940	-2.089	758.1502	-2.116	767.2266	-1.887	802.0216	-1.183	803.0779	-1.577
741.0976	-2.098	758.1534	-2.101	767.2294	-1.914	802.0243	-1.215	803.0818	-1.681
741.1012	-2.077	758.1599	-2.039	770.1473	-1.956	802.0299	-1.422	803.0896	-1.849
741.1086	-2.037	758.1631	-2.074	770.1528	-2.035	802.0356	-1.621	803.0931	-1.918
741.1123	-2.003	758.1696	-1.975	770.1591	-2.062	802.0383	-1.690	803.1071	-2.076
741.1160	-1.957	758.1892	-1.650	770.1649	-2.109	802.0411	-1.806	803.1105	-2.089
741.1198	-1.888	758.1956	-1.416	770.1762	-2.107	802.0438	-1.847	803.1176	-2.120
741.1235	-1.827	758.2022	-1.385	770.1975	-2.162	802.0672	-2.075	803.1212	-2.147
741.1272	-1.730	758.2086	-1.551	770.2076	-2.009	802.0699	-2.104	803.1248	-2.162
741.1310	-1.649	758.2119	-1.656	770.2129	-1.879	802.0726	-2.080	803.1282	-2.160
741.1347	-1.517	758.2314	-2.051	770.2182	-1.696	802.0753	-2.121	803.1317	-2.151
741.1384	-1.414	758.2411	-2.051	770.2288	-1.314	802.0780	-2.096	803.1385	-2.130
741.1422	1.408	767.0364	2.070	770.2394	1.231	802.0807	2.121		
741.1459	1.464	767.0394	2.069	770.2447	1.330	802.0835	2.094		
741.1496	1.569	767.0571	1.879	774.1166	1.941	802.0862	2.081		
741.1570	1.754	767.0630	1.812	774.1187	1.960	802.0889	2.117		
743.0000	1.652	767.0693	1.668	774.1240	2.022	802.0916	2.089		
743.0044	1.515	767.0835	1.432	774.1275	2.071	802.0943	2.058		
743.0450	2.053	767.0870	1.510	774.1362	2.097	802.0971	2.039		
743.0560	2.104	767.0905	1.580	774.1509	2.157	802.0998	2.035		
743.0613	2.163	767.0976	1.740	774.1541	2.122	802.1025	2.010		
743.0659	2.133	767.1046	1.878	774.1557	2.131	802.1053	2.009		

$$Min\ I = JD_{\odot}2454767.1987 + 0.^{d}23369722\ E,$$

where the period of $0.^{d}23369722$ is adopted from Jeong et al. (2006) and the epoch of $JD_{\odot}2454767.1987$ from ours (in Table 4).

It is remarkable that magnitude at the outside-eclipse phase of 0.2-0.3 is quite different to that of 0.7-0.8 in the light curve of Fig. 1. Zhai et al. (1988) explained such an asymmetry is due to the spot activity on the secondary component. The variation in the light curves of V523 Cas takes place in terms of days, weeks, and months. In order to see the figure of variations in residuals (observed minus averaged), Genet et al. (2005) obtained a master light curve (M-curve) by means of phase-binned analysis of their 21248 observations.

3. LIGHT CURVE SOLUTION

We analyzed the light curves of V523 Cas using WD program (Wilson & Devinney 1971, Wilson & van Hamme 2004). For the input data, we made about 50 normal points from our data in each filter, and made the data which are converted from the M-curve of Genet et al. (2005). Mode 3 and model atmosphere were applied. We used g, T_2, A, and q as fixed parameters and i, T_1, Ω_1,

Table 3. R observations of V523 Cas in 2008.

$JD_{\odot}$ 2450300+	ΔR	$JD_{\odot}$ 2450300+	ΔR	$JD_{\odot}$ 2450300+	ΔR	$JD_{\odot}$ 2450300+	ΔR	$JD_{\odot}$ 2450300+	ΔR
739.0895	2.383	743.1398	1.784	758.2286	2.264	774.1172	2.207	802.0893	2.321
739.0933	2.417	758.0466	2.305	767.0400	2.309	774.1192	2.242	802.0920	2.329
739.1160	2.306	758.0531	2.253	767.0429	2.287	774.1209	2.257	802.0948	2.332
739.1224	2.266	758.0564	2.203	767.0488	2.262	774.1226	2.276	802.0975	2.294
739.1255	2.213	758.0596	2.199	767.0606	2.107	774.1261	2.299	802.1002	2.305
739.1287	2.187	758.0628	2.090	767.0665	2.013	774.1295	2.342	802.1029	2.247
739.1318	2.153	758.0693	1.919	767.0771	1.746	774.1348	2.365	802.1057	2.239
739.1350	2.070	758.0791	1.527	767.0877	1.795	774.1416	2.390	802.1084	2.197
739.1381	1.990	758.0823	1.466	767.0912	1.885	774.1432	2.396	802.1111	2.203
739.1444	1.742	758.0856	1.465	767.0947	1.946	774.1448	2.426	802.1138	2.140
739.1581	1.498	758.0921	1.631	767.1088	2.214	774.1544	2.413	802.1165	2.095
739.1739	1.985	758.0954	1.729	767.1159	2.291	774.1576	2.398	802.1195	2.021
739.2133	2.353	758.0986	1.833	767.1256	2.355	774.1592	2.385	802.1225	1.979
741.0739	2.330	758.1019	1.925	767.1283	2.378	774.1919	2.021	802.1254	1.879
741.0773	2.335	758.1052	2.056	767.1310	2.370	774.1976	1.877	802.1284	1.801
741.0805	2.366	758.1084	2.068	767.1337	2.368	774.2108	1.533	802.1313	1.735
741.0838	2.364	758.1116	2.138	767.1365	2.374	774.2252	1.966	802.1343	1.732
741.0874	2.348	758.1182	2.212	767.1401	2.399	774.2323	2.113	802.1372	1.703
741.0909	2.352	758.1246	2.276	767.1430	2.396	774.2393	2.185	802.1402	1.755
741.0946	2.344	758.1279	2.252	767.1655	2.245	801.9991	2.022	802.1461	1.979
741.1018	2.312	758.1344	2.394	767.1790	2.004	802.0012	1.937	802.1520	2.085
741.1092	2.269	758.1376	2.318	767.1847	1.870	802.0034	1.893	802.1549	2.132
741.1129	2.259	758.1409	2.321	767.1931	1.546	802.0057	1.822	803.0404	2.255
741.1203	2.153	758.1441	2.346	767.2072	1.687	802.0132	1.541	803.0467	2.175
741.1278	1.978	758.1506	2.425	767.2128	1.881	802.0193	1.475	803.0533	2.052
741.1352	1.777	758.1538	2.380	767.2157	1.954	802.0220	1.462	803.0565	1.996
741.1427	1.706	758.1571	2.376	767.2185	2.028	802.0248	1.559	803.0598	1.898
741.1464	1.761	758.1603	2.351	767.2327	2.226	802.0303	1.736	803.0632	1.793
741.1502	1.863	758.1635	2.332	767.2355	2.279	802.0360	1.969	803.0669	1.713
741.1538	1.983	758.1668	2.275	770.1482	2.246	802.0388	2.007	803.0747	1.766
741.1576	2.045	758.1701	2.209	770.1538	2.268	802.0415	2.046	803.0786	1.855
743.0049	1.785	758.1733	2.209	770.1600	2.321	802.0442	2.129	803.0825	1.942
743.0225	1.947	758.1798	2.058	770.1659	2.349	802.0676	2.320	803.0864	2.050
743.0343	2.185	758.1831	2.018	770.1715	2.359	802.0703	2.324	803.0901	2.147
743.0456	2.282	758.1863	2.028	770.1769	2.430	802.0730	2.334	803.0935	2.204
743.0565	2.366	758.1961	1.708	770.2081	2.231	802.0757	2.334	803.1004	2.282
743.0663	2.381	758.2026	1.745	770.2134	2.179	802.0784	2.353	803.1041	2.312
743.0743	2.412	758.2058	1.754	770.2187	2.051	802.0812	2.360	803.1075	2.331
743.0946	2.282	758.2091	1.858	770.2346	1.510	802.0839	2.359	803.1109	2.353
743.1039	2.150	758.2123	1.941	774.1120	2.120	802.0866	2.389	803.1145	2.379

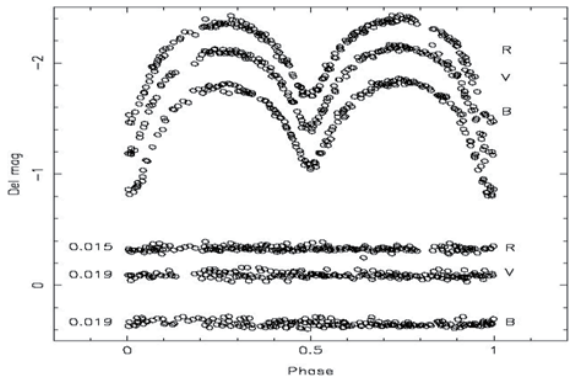

Fig. 1. Light curves of V523 Cas in 2008.

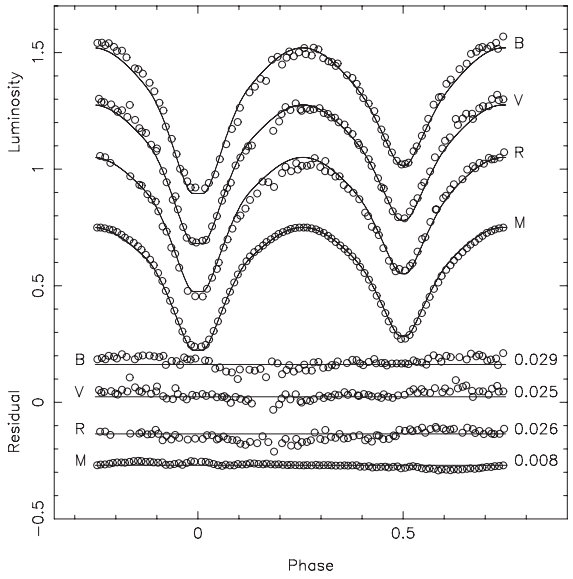

Fig. 2. Light curves of V523 Cas in 2008. Solid lines stand for the model without spots.

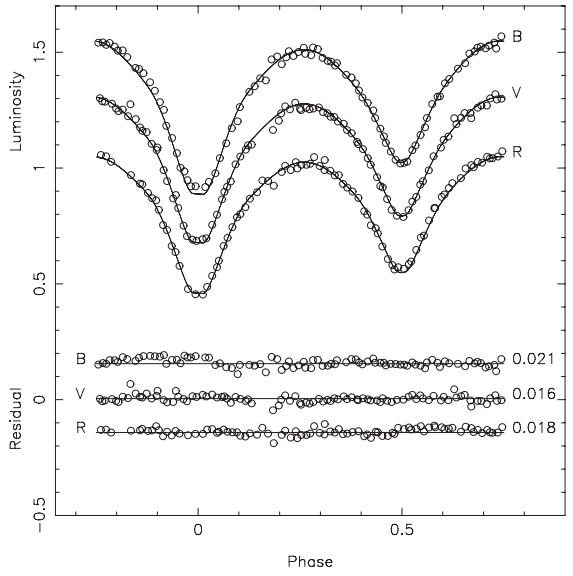

Fig. 3. Light curves of V523 Cas in 2008. Solid lines stand for the model with spots.

L_1, Lat_{sopt}, $Long_{sopt}$ as adjustable parameters. The values for fixed parameters and the initial values for adjustable parameters are adopted from Jeong et al. (2006) and van Hamme (1993).

Table 4. Times of minimum light of V523 Cas.

Min I $JD_{\odot}$2454000+	p.e.	Min II $JD_{\odot}$2454000+	p.e.
758.0857	±0.0004	741.1415	±0.0002
767.1987	±0.0002	758.2001	±0.0006
802.0390	±0.0004	767.0819	±0.0005
		741.1415	±0.0004
		758.2001	±0.0003
		767.0819	±0.0004

Table 5. Light curve solutions of V523 Cas.

Parameter	Samec et al. (2004)	Jeong et al. (2006)	This paper
a ($R_{\odot}$)	1.687 ± 0.012	1.687 ± 0.005	1.687 ± 0.005
V_0 (km/s)	-3.6 ± 0.6	-2.5 ± 0.5	-2.5 ± 0.5
Φ	0.0000 ± 0.0017[a]	-0.0004 ± 0.0003	-0.0004 ± 0.0003
$A_{1,2}$	0.5	0.5	0.5
I	85.39 ± 0.11	85.02 ± 0.20	85.080 ± 0.25
T_1 (K)	5,104 ± 2[a]	5,156 ± 2.2	5082 ± 8.5
T_2 (K)	4,762 ± 102[a]	4,763 ± 1.8	4763 ± 1.8
$q = M_1/M_2$	1.923 ± 0.002[a]	1.840 ± 0.007	1.761 ± 0.019
$\Omega_1 = \Omega_2$		4.868 ± 0.004	4.787 ± 0.029
$g_{1,2}$	0.32	0.32	0.32
x $(B)_{1,2}$	0.799, 0.799	0.842, 0.830	0.842, 0.830
y $(B)_{1,2}$	0.149, 0.149	-0.161, -0.176	-0.161, -0.176
x $(V)_{1,2}$	0.799, 0.799	0.803, 0.801	0.803, 0.801
y $(V)_{1,2}$	0.149, 0.149	0.001, -0.006	0.001, -0.006
x $(R)_{1,2}$		0.736, 0.747	0.736, 0.747
y $(R)_{1,2}$		0.108, 0.105	0.108, 0.105
x $(I)_{1,2}$		0.639, 0.648	
y $(I)_{1,2}$		0.156, 0.164	
$L_1 = (L_1 + L_2)_B$	0.550 ± 0.024	0.515 ± 0.02	0.496 ± 0.0005
$L_1 = (L_1 + L_2)_V$	0.527 ± 0.025	0.485 ± 0.02	0.472 ± 0.0001
$L_1 = (L_1 + L_2)_R$		0.457 ± 0.02	0.449 ± 0.0003
$L_1 = (L_1 + L_2)_I$		0.441 ± 0.02	
r_1 (pole)	0.4263 ± 0.0004[a]	0.3211 ± 0.0005	0.3172 ± 0.0034
r_1 (side)	0.4560 ± 0.0005[a]	0.3377 ± 0.0006	0.3329 ± 0.0041
r_1 (back)	0.4909 ± 0.0006[a]	0.3806 ± 0.0012	0.3721 ± 0.0071
r_2 (pole)	0.3186 ± 0.0012[a]	0.4217 ± 0.0002	0.4164 ± 0.0029
r_2 (side)	0.3352 ± 0.0014[a]	0.4504 ± 0.0003	0.4437 ± 0.0038
r_2 (back)	0.3352 ± 0.0014[a]	0.4851 ± 0.0006	0.4764 ± 0.0054
Lat $(spot)_1$	117 ± 2[a]	90.0	90.0
Long $(spot)_1$	7 ± 0.7[a]	285.0	120.91 ± 9.3
R $(spot)_1$	18 ± 1[a]	19.0	13.1 ± 1.0
T.F. $(spot)_1$	1.165 ± 0.015[a]	0.9	1.11 ± 0.1
Lat $(spot)_2$		90.0	90.0
Long $(spot)_2$		65.0	134.1 ± 1.6
R $(spot)_2$		112	10
T.F. $(spot)_2$		1.1	0.7
Fill-out factor (%)	29 ± 2	26.9	21.6
$\sum\omega$ $(o\text{-}c)^2$	0.054797	0.0377395	0.0305819

[a]converted from the original data because Samec et al. (2004) used a hot component as star 2 while we used a hot component as star 1

Two solutions were obtained because the luminosity at the 0.75 phase is much higher than that at 0.25. First, we executed WD differential correction code iteratively, and tried to obtain the best fitting to *BVR* curves and M-curve, simultaneously, without any spot, where the sum of weighted square residuals is $\sum w\ (O\text{-}C)^2 = 0.0319741$. Next we tried to fit the model with *BVR* curves without M-curve and with two spots, one spot is cool ($f = 0.7$) at $Long = 135^{\circ}$ and $Lat = 90^{\circ}$ on the secondary component and other one with a hot spot near $Long = 120^{\circ}$ and $Lat = 90^{\circ}$ on the primary component, and as fixed parameters we used the results of first solution. In this case, the sum of weighted square residuals $\sum w\ (O\text{-}C)^2 = 0.0305819$ (see 4th column of Table 5). The results of spot parameters are listed in the lower part of the 4th column of Table 5. In order to compare, the solutions by Samec et al. (2004) and Jeong et al. (2006) are also tabulated in the 2nd and 3rd columns of Table 5, respectively.

The synthetic light curves according to our solutions are constructed as shown in Figs. 2 and 3, respectively. On the upper part of those figures, the open circles stand for normal points of our observations and solid lines for the calculated light curves. On the bottom part, together with a plot of the residuals (observed minus modeled) and their probable errors. It is clear that the model light curves with spots (in Fig. 3) better fit the observations than those without spots (in Fig. 2). Probable errors are 0.029 for *B*, 0.025 for *V*, 0.026 for *R*, and 0.008 for M-curve as shown in Fig. 2. In the second trial, probable errors are

Table 6. Absolute dimension of the V523 Cas system.

Source	$M_1/M_{\odot}$	$M_2/M_{\odot}$	$R_1/R_{\odot}$	$R_2/R_{\odot}$	$M_{bol,1}$	$M_{bol,2}$
Samec et al. (2004)	0.40	0.78	0.58	0.78	6.49	6.18
Kim & Jeong (2002)	0.32	0.54	0.52	0.66	...	...
Jeong et al. (2006)	0.42	0.77	0.59	0.77	6.38	6.11
Latkovic et al. (2009)	0.40	0.78	0.57	0.76	6.48	6.21
This paper	0.43	0.76	0.59	0.76	6.41	6.14

Table 7. Over contact factors of V523 Cas system.

Observing season year/month	Fill-out factor (%)	Source
1998/09	29	Samec et al. (2004)
1999/10	0.13	Kim & Jeong (2002)
2003/01	26.9	Jeong et al. (2006)
2005/09	4.82	Zboril & Djurasevic (2006)
2006/09	20.0	Latkovic et al. (2009)
2008/09-10	21.6	This paper

much improved as 0.021 for *B*, 0.016 for *V*, 0.018 for *R* as shown in Fig. 3. Using the equation of $f = (\Omega_{in} - \Omega) / (\Omega_{in} - \Omega_{out})$, a fill-out factor of $f = 21.6\%$ is calculated. The absolute dimensions for the V523 Cas system are obtained and listed with data published as shown in Table 6. Assuming the component stars of V523 Cas are synchronously rotating, their rotation velocities of 125 km/s and 161 km/s are estimated from $R_1 = 0.59R_\odot$ and $R_2 = 0.76R_\odot$.

4. DISCUSSION

Our solution for the V523 Cas system exhibits that the massive, bright and larger component is cooler (see Table 6), and it has a common envelope (fill-out factor 21.6%) but the temperatures of the two components are different (~300 K). According to the published solutions (including ours) for V523 Cas, the position, size and temperature of spots are rapidly changing, and affect light variation. Those observational evidences for V523 Cas are reflecting the existence of very strong magnetic fields due to both their rapid rotation (dynamo effect) and their low temperature, which makes generally deep convective envelopes with long convective turnover times (Rucinski 1993). But most late single stars which are slowly rotating, are not very active, magnetically.

How to keep such a state of a common envelope with two components which have different temperatures? Recently, Kiuchi et al. (2010) present a new formula to numerically construct configuration in rotational equilibrium, which consist of multiple layers. The multiple-layer rapid rotation system may keep such a disequilibrium state. Then the common envelope should be relatively thin disequilibrium. Of course such a mechanism makes envelope unstable and causes some variation in envelope depth. The fill-out factor could be an indicator of envelope depth because it is said 'over contact' when its factor is positive. In the short term period, variation of the envelope depth may be caused by another sub mechanism during the long term journey of the TRO evolution procedure. We collect the fill-out factors from published literature and listed in Table 7. It shows that the factors are changed over short terms period such as a decade.

Despite great progress, many problems remain to be studied. Genet et al. (2005) insisted on the necessity of high precision observation. Until now, our observations are like snapshots of W UMa systems, but nowadays with highly developed technology we can provide movies of their behavior over daily, monthly and yearly timescales. This would enable more powerful feedback on the theoretical models and, ultimately, a better understanding of over-contact binary structure and evolution.

ACKNOWLEDGEMENTS

This work was supported by the research grant of the Chungbuk National University in 2008. We are very grateful to Dr. R. E. Wilson for allowing us to use his new W-D code.

REFERENCES

Applegate, J. H. 1992, ApJ, 385, 621, doi: 10.1086/170967
Bradstreet, D. H. 1981, AJ, 86, 98, doi: 10.1086/112861
Flannery, B. P. 1976, ApJ, 205, 217, doi: 10.1086/154266
Genet, R. M., Smith, T. C., Terrell, D., & Doyle, L. 2005, in 24th Annual Symposium on Telescope Science (Big Bear Lake, CA: Society for Astronomical Sciences), p.45
Haussler, K. 1974, IBVS, 887, 1
Hendry, P. D. & Mochnacki, S. W. 2000, ApJ, 531, 467, doi: 10.1086/308427
Hoffmann, M. 1981, IBVS, 1976, 1
Jeong, J. H., Kim, C. H., & Lee, Y. S. 2006, JASS, 23, 177
Jeong, J. H., Kim, C. H., Lee, Y. S., & Yoon, Y. N. 2009, JASS, 26, 157
Kim, J. H. & Jeong, J. H. 2002, JASS, 19, 263
Kiuchi, K., Nagakura, H., & Yamada, S. 2010 May 13, Astrophysics (astro-ph), eprint arXiv:1005.2236
Kwee, K. K. & van Woerden, H. 1956, BAN, 12, 327
Latkovic, O., Zboril, M., & Djurasevic, G. 2009, SerAJ, 178, 45, doi: 10.2298/SAJ0978045L
Lavrov, M. I. & Zhukov, G. V. 1975, ATsir No. 873, 1
Lister, T. A., McDermid, R. M., & Hilditch, R. W. 2000, MNRAS, 317, 111, doi: 10.1046/j.1365-8711.2000.03552.x
Lucy, L. B. 1976, ApJ, 205, 208, doi: 10.1086/154265
Milone, E. F., Hrivnak, B. J., & Fisher W. A. 1985, AJ, 90, 354, doi: 10.1086/113739
Niarchos, P. G. & Duerbeck, H. W. 1991, A&A, 247, 399
Robertson, J. A. & Eggleton, P. P. 1977, MNRAS 179, 359
Rucinski, S. M. 1993, in The Realm of Interacting Binary Stars, eds. J. Sahade, G. E. McCluskey, & Y. Kondo (Boston: Kluwer Academic Publishers), pp.111-142
Rucinski, S. M., Capobianco, C. C., Lu, W., DeBond, H., Thomson, J. R., Mochnacki, S. W., Blake, R. M., Ogloza, W., Stachowski, G., & Rogoziecki, P. 2003, AJ, 125, 3258, doi: 10.1086/374949
Samec, R. G. & Bookmyer, B. B. 1987, IBVS, 2986, 1
Samec, R. G., Faulkner, D. R., & Wiliams, D. B. 2004, AJ, 128,

2997, doi: 10.1086/426357
Samec, R. G., van Hamme, W., & Bookmyer, B. B. 1989, AJ, 98, 2287, doi: 10.1086/115299
van Hamme, W. 1993, AJ, 106, 2096, doi: 10.1086/116788
Weber, R. 1958, JO, 41, 74.
Wilson, R. E. 1978, ApJ 224, 885, doi: 10.1086/156438
Wilson, R. E. & Devinney, E. J. 1971, ApJ, 166, 605, doi: 10.1086/150986
Wilson, R. E. & van Hamme, W. 2004 (Revision of November, 2007), Computing Binary Star Observables [Electronic Document] Available from: ftp://ftp.astro.ufl.edu/pub/wilson/lcdc2007/ebdoc2007.pdf.gz
Zboril, M. & Djurasevic, G. 2006, SerAJ, 173, 89, doi: 10.2298/SAJ0673089Z
Zhai, D. S., Zhang, W. Y., & Lu, W. X. 1988, Ap&SS, 146, 1, doi: 10.1007/BF00656975
Zhukov, G. V. 1972, ATsir, 668, 7